To: Dr. Saundra F. DeLauder, Dean of Graduate Studies and Research

The members of the Committee approved the Thesis of Jason M Cornelius as presented on July 7, 2015.

We recommend that it be accepted in partial fulfillment of the requirements for the degree of Master of Science with a major in Applied Mathematics.

Dr. Jinjie Liu, Advisor	Department of Mathematical Sciences	Date 7/10/2015
Dr. Fengshan Liu, Member	Department of Mathematical Sciences	Date 7/7/15
Dr. Matthew Tanzy, Member	Department of Mathematical Sciences	Date 7/7/2015
Dr. Moysey Brio Outside Member	Department of Mathematics, The University of Arizona	Date 7/7/15

APPROVED

Dr. Jinjie Liu, Program Director	Department of Mathematical Sciences	Date 7/10/2015
Dr. Noureddine Melikechi, Dean	College of Mathematics, Natural Sciences and Technology	Date 7/13/15
Dr. Saundra F. DeLauder, Dean	School of Graduate Students and Research	Date 7/17/2015

FINITE-DIFFERENCE TIME-DOMAIN ALGORITHM FOR MAGNETO-ELECTRIC MATERIALS AND THE SPACE-TIME CLOAK

by

JASON CORNELIUS

A THESIS

Submitted in partial fulfillment of the requirements for the degree of
Master of Science in the Applied Mathematics Graduate
Program of Delaware State University

DOVER, DELAWARE
August 2015

COPYRIGHT

DEDICATION

This work is dedicated to my family, friends and colleagues. Their continued support has played a pivotal role in faciliating the completion of this academic milestone.

ACKNOWLEDGEMENTS

I would like to thank my advisor, Dr. Jinjie Liu. Without his support and guidance this work would not have been possible. I would also like to thank the members of my defense committee, Dr. Jinjie Liu, Dr. Fenghshan Liu, Dr. Moysey Brio and Dr. Matthew Tanzy for their valuable feedback and encouragement during the writing and defense of this thesis. Additionally, I would also like to thank the Department of Mathematics at Delaware State University as a whole for supporting and facilitating my research endeavors. Lastly, I would like to acknowledge the US DoD ARO Grant W911NF-11-2-0046 and the US AFOSR Grant FA9550-10-1-0127 for their support.

ABSTRACT

In this work, we conduct a review of electromagnetics and the traditional FDTD method for isotropic media. We analyze the pitfalls and shortcomings of this method when it comes to the approximation of electromagnetic wave propagation through more exotic media, such as anisotropic media and magnetoelectric media with time and space varying permittivity, permeability and coupling coefficients. For the latter medium we present an extension to FDTD that utilizes a dual grid structure to overcome the late-time instability associated with conventional extrapolation based extensions to FDTD. We apply both of these methods to the simulation of the space-time cloak and analyze the stability of both.

TABLE OF CONTENTS

TITLE PAGE i
COPYRIGHT
DEDICATION ii
ACKNOWLEDGEMENTS iii
ABSTRACT iv
TABLE OF CONTENTS v

LIST OF FIGURES OR ILLUSTRATIONS vii
LIST OF TABLES viii
CHAPTER 1 INTRODUCTION 1
CHAPTER 2 ELECTROMAGNETICS AND FDTD 3
2.1 Maxwell's Equations 3
2.1.1 Material Response 4
2.1.2 Maxwell's Equation in 2D 6
2.1.3 Maxwell's Equation in 1D 7
2.2 FDTD 7
2.2.1 FDTD Algorithm 8
2.2.2 FDTD for Anistropic media 11
CHAPTER 3 TRANSFORMATION OPTICS AND MAGNETO-ELECTRIC MEDIA 14
3.1 Transformations of Maxwell's Equations 14
3.1.1 Transformed material parameters for spatial transformations . 17
3.1.2 Material parameters for a 1D space-time transformation (1+1D) 18
3.2 The conventional FDTD method for time dependent magneto-electric medium 19
3.3 The overlapping Yee Algorithm for time dependent magneto-electric media 22
CHAPTER 4 SIMULATION OF THE SPACETIME CLOAK . . . 25
4.1 Transformation Optics and space-time cloak 25
4.2 Simulation of the space-time cloak 26
4.3 Stability Analysis 29
CHAPTER 5 CONCLUSION AND FUTURE WORK 32
5.1 Conclusion 32
5.2 Future Work 32

REFERENCE LIST **34**
CURRICULUM VITAE **36**

LIST OF FIGURES OR ILLUSTRATION

2.1 Cell location at index (i,j) 9

2.2 Stable averaging scheme for anisotropic media 12

3.1 Computation of $\bar{E}_z$ using (a) the time extrapolation under a conventional FDTD method and (b) the overlapping Yee algorithm without extrapolation. 22

4.1 (a) A spacetime cloak in the (t, x) domain. (b) Free space after the transformation to the (τ, ξ) domain. 26

4.2 Contour plots of the electric field intensity for spacetime cloak simulations. Left column: results using a conventional time extrapolation based FDTD method with grid sizes a) $N = 1600$, (c) $N = 2000$, and (e) $N = 2400$, respectively. Right column: the corresponding results using the overlapping Yee FDTD method. . . 28

4.3 Evolution of the Electric field as the wave propagates through the spacetime cloak. 29

4.4 Distribution of the eigenvalues in the complex plane for (a) the overlapping Yee FDTD method and (b) the conventional FDTD method. 30

LIST OF TABLES

2.1 Permittivity and Permeability for some materials 4

Chapter 1

INTRODUCTION

In recent years, Transformation Optics (TO) has become one of more interesting topics in science. Utilizing transformation optics and meta-materials, spatial invisibility cloaks [5, 9] have been developed. Designs such as these have been physically realized at microwave frequencies [11] and optical frequencies [15]. A spatial cloak functions by manipulating the spatial path of electromagnetic waves within the cloaked region in such a way that waves are bent around the object being cloaked. Transformation optics allows for a description of the medium (ie: material parameters) needed for the construction of such devices. For this particular type of cloak, the implementation requires the use of inhomogeneous media where the inhomogeneity is due to the use of spatially dependent anisotropic permeability and permittivity.

Within the past several years, a new type of cloak has been developed [4, 8], the space-time cloak. Contrary to the spatial cloak, a space-time cloak functions by altering the speed of the electromagnetic wave as it propagates through the cloaked region. Initially, the speed of the front of the wave is increased while the speed of the back of the wave is decreased. This allows for a gap to occur in which an event, or subset of the space-time plane, can be carried out undetected. To close the gap, the back of the wave is sped up and the front is slowed down allowing the wave to continue on at its original speed. This effect has been experimental demonstrated in the work in [3].

The design of such a cloak can be achieved by transformation optics, and it results in a magneto-electric medium with time and space varying permittivity, permeability, and coupling coefficient [8].

Due to the interesting nature of these devices, simulation is desirable. In this work, we are interested in simulating space and time dependent magneto-electric materials and their direct application to the space-time cloak. In [4], the FDTD method has been applied to simulate the space-time cloak but the authors point out that there are some difficulties near the closing process of the space-time cloak. Our numerical simulations demonstrate that there are instabilities for conventional FDTD simulation due to the temporal extrapolation of the time dependent magneto-electric constitutive equations.

We begin the body of this work by discussing some of the foundations of Electromagnetics, the FDTD method (Chapter 2) and Transformation Optics (Chapter 3). Also in Chapter 3, we look at an extrapolation based method and present a modified FDTD method based on time overlapped grids for handling magneto-electric media. Our method utilizes two Yee grids that are offset in time by a halfstep so that collocated fields are provided to the time-dependent magneto-electric constitutive equations. This method avoids time extrapolation and the it's associated instabilities. In Chapter 4, we provide a simulation of the space-time cloak as a numerical example. Lastly, in Chapter 5, we give some concluding remarks and discuss some possible future work.

Chapter 2

ELECTROMAGNETICS AND FDTD

2.1 Maxwell's Equations

Electromagnetic waves propagate through the generation and oscillation of electric and magnetic fields. When considering the propagation of electromagnetic waves in a linear medium, the governing equations are a set of partial differential equations known as Maxwell's Equations. The first two laws describe the interaction between time-changing electric and magnetic fields

$$\frac{\partial \mathbf{B}}{\partial t} = -\nabla \times \mathbf{E}, \tag{2.1}$$

$$\frac{\partial \mathbf{D}}{\partial t} = \nabla \times \mathbf{H} - \mathbf{J}, \tag{2.2}$$

while the last two laws describe the impact of electrical and magnetic charges on electrical and magnetic fields.

$$\nabla \cdot \mathbf{D} = \rho, \tag{2.3}$$

$$\nabla \cdot \mathbf{B} = 0. \tag{2.4}$$

In the above $\mathbf{E}$ and $\mathbf{H}$ are the electric and magnetic fields while $\mathbf{D}$ and $\mathbf{B}$ are the electric and magnetic flux densities associated with material's electrical and magnetic response. $\mathbf{J}$ and ρ are the current and charge densities respectively. These equations are named, Faraday's Law of Induction, Ampere-Maxwell's Law, Gauss's Law of Electric Fields and Gauss's Law of Magnetism respectively. Faraday's Law,

equation (2.1), states that an electrical field is generated by a changing magnetic field. Ampere's Maxwell's Law, equation (2.2), states that a magnetic field can be generated from either a changing electric field or a current source. Gauss's Law of Electrical Fields, equation (2.3), states that Electric field lines extend outward from positive charges while Gauss's Law of Magnetism, equation (2.4), states there are no magnetic charges (ie: there are no magnetic monopoles)

2.1.1 Material Response

When an electromagnetic wave propagates through a medium (whether it be a vacuum or dielectric) an electromagnetic response is exhibited based on that material's electrical and magnetic properties. For linear isotropic materials, materials whose response is independent of electromagnetic wave's angle of incidence, this response is dictated by the material's electrical permittivity (ϵ) and magnetic permeability (μ). In essence, these parameters describe how easily a electric field or magnetic field is setup inside of a given materials. In a vacuum these parameters are $\epsilon_0 = 8.854187 \times 10^{-12} F \cdot m^{-1}$ and $\mu_0 = 1.256637 \times 10^{-6} H \cdot m^{-1}$. In most cases, the parameters for other materials are given relative to these values using the relation $\epsilon = \epsilon_r \cdot \epsilon_0$ and $\mu = \mu_r \cdot \mu_0$. Some typical permittivities and permeabilities are given in Table 2.1 [6].

Material	Permitivity	Permeability
Vacuum	1	1
Air	1.00053	1.000006
Silicon Rubber	3.12	1
Water at 20C	80.100	1
Iron		25000

Table 2.1: Permittivity and Permeability for some materials

These physical parameters bring about the relationship between the field quantities $\mathbf{D}$ and $\mathbf{E}$ as well as $\mathbf{B}$ and $\mathbf{H}$. This relationship is given by the so called constitutive relations. For linear isotropic materials we have

$$\mathbf{D} = \epsilon \mathbf{E}, \tag{2.5}$$

$$\mathbf{B} = \mu \mathbf{H}. \tag{2.6}$$

For materials, called anisotropic, whose response is dependent upon the orientation of the electric field, the material properties take on the tensor form

$$\hat{\epsilon} = \begin{pmatrix} \epsilon_{xx} & \epsilon_{xy} & \epsilon_{xz} \\ \epsilon_{yx} & \epsilon_{yy} & \epsilon_{yz} \\ \epsilon_{zx} & \epsilon_{zy} & \epsilon_{zz} \end{pmatrix}, \qquad \hat{\mu} = \begin{pmatrix} \epsilon_{xx} & \epsilon_{xy} & \epsilon_{xz} \\ \epsilon_{yx} & \epsilon_{yy} & \epsilon_{yz} \\ \epsilon_{zx} & \epsilon_{zy} & \epsilon_{zz} \end{pmatrix}. \tag{2.7}$$

In materials of this type waves interact with the medium differently depending on their angle of incidence.

Lastly, in more exotic media, magneto-electric materials, these constitutive relations may become coupled and yield the matrix (or block matrix) equation

$$\begin{pmatrix} \mathbf{D} \\ \mathbf{B} \end{pmatrix} = \begin{pmatrix} \epsilon & \xi \\ \bar{\xi} & \mu \end{pmatrix} \begin{pmatrix} \mathbf{E} \\ \mathbf{H} \end{pmatrix}, \tag{2.8}$$

where ϵ, μ and ξ are scalar or tensor depending on whether the material is isotropic or anisotropic. For all of these classifications the material may also be homogeneous or inhomogeneous. Inhomogeneous materials are materials which have permittivities,

permeabilities, or coupling coefficients that vary spatially throughout the material. Homogeneous materials, have parameters which remain constant with respect to the spatial variables.

When considering numerical schemes it is useful to have Maxwell's Equations in component form. We consider the 2-D and 1-D cases as they are most relevant to this work.

2.1.2 Maxwell's Equation in 2D

Considering the case where there is no variation in the z-direction and expanding the curl equations (Ampere-Maxwell's and Faraday's law), we obtain

$$\begin{pmatrix} \frac{\partial \mathbf{D_x}}{\partial t} \\ \frac{\partial \mathbf{D_y}}{\partial t} \\ \frac{\partial \mathbf{D_z}}{\partial t} \end{pmatrix} = \begin{pmatrix} \frac{\partial \mathbf{H_z}}{\partial y} \\ -\frac{\partial \mathbf{H_z}}{\partial x} \\ \frac{\partial \mathbf{H_y}}{\partial x} - \frac{\partial \mathbf{H_x}}{\partial y} \end{pmatrix} \tag{2.9}$$

and

$$\begin{pmatrix} \frac{\partial \mathbf{B_x}}{\partial t} \\ \frac{\partial \mathbf{B_y}}{\partial t} \\ \frac{\partial \mathbf{B_z}}{\partial t} \end{pmatrix} = \begin{pmatrix} -\frac{\partial \mathbf{E_z}}{\partial y} \\ \frac{\partial \mathbf{E_z}}{\partial x} \\ \frac{\partial \mathbf{E_x}}{\partial y} - \frac{\partial \mathbf{E_y}}{\partial x} \end{pmatrix}. \tag{2.10}$$

This yields two distinct systems of partial differential equation. The first is known as the Transverse Electric (TE_z) Mode

$$\begin{pmatrix} \frac{\partial \mathbf{D_x}}{\partial t} \\ \frac{\partial \mathbf{D_y}}{\partial t} \\ \frac{\partial \mathbf{B_z}}{\partial t} \end{pmatrix} = \begin{pmatrix} \frac{\partial \mathbf{H_z}}{\partial y} \\ -\frac{\partial \mathbf{H_z}}{\partial x} \\ \frac{\partial \mathbf{E_x}}{\partial y} - \frac{\partial \mathbf{E_y}}{\partial x} \end{pmatrix} \tag{2.11}$$

while the second is known as the Transverse Magnetic (TM_z) Mode

$$\begin{pmatrix} \frac{\partial \mathbf{B_x}}{\partial t} \\ \frac{\partial \mathbf{B_y}}{\partial t} \\ \frac{\partial \mathbf{D_z}}{\partial t} \end{pmatrix} = \begin{pmatrix} -\frac{\partial \mathbf{E_z}}{\partial y} \\ \frac{\partial \mathbf{E_z}}{\partial x} \\ \frac{\partial \mathbf{H_y}}{\partial x} - \frac{\partial \mathbf{H_x}}{\partial y} \end{pmatrix}. \tag{2.12}$$

2.1.3 Maxwell's Equation in 1D

Lastly, if we consider Maxwell's equations in 1-D, both field quantities are transverse to the direction of propagation. In this case we are left with two sets of two equations, depending on how we wish to orient the electric field. For the z-polarized equations (electric field pointing in the z-direction) we have

$$\begin{pmatrix} \frac{\partial \mathbf{D_z}}{\partial t} \\ \frac{\partial \mathbf{B_y}}{\partial t} \end{pmatrix} = \begin{pmatrix} \frac{\partial \mathbf{H_y}}{\partial x} \\ \frac{\partial \mathbf{E_z}}{\partial x} \end{pmatrix} \tag{2.13}$$

and for the y-polarization we have

$$\begin{pmatrix} \frac{\partial \mathbf{D_y}}{\partial t} \\ \frac{\partial \mathbf{B_z}}{\partial t} \end{pmatrix} = \begin{pmatrix} -\frac{\partial \mathbf{H_z}}{\partial x} \\ -\frac{\partial \mathbf{E_y}}{\partial x} \end{pmatrix}. \tag{2.14}$$

2.2 FDTD

The FDTD method [12, 13, 19] is a very successful method for simulating electromagnetic wave propagation. It has been applied to the study of various types of materials [13, 14], including dielectrics, linear dispersive materials, nonlinear Raman and Kerr materials, nonlinear dispersive materials [7], bi-isotropic media [1, 10], etc.

FDTD is a numerical scheme that utilizes a staggered grid and central differences to approximate the time and spatial derivative operators present in Maxwell's equations. This numerical scheme achieves second order accuracy in space and time.

2.2.1 FDTD Algorithm

We consider the algorithm in 2-D applied to the TE_z mode equations, equation 2.11, as presented in [13] with the only exception being that isotropic constitutive relations are not substituted into the formulation. First, we truncate the propagation region to a finite region of interest which is known as the computational domain. In the 2-D case this region is a rectangular subset of the cartesian plane. Next this domain is discretized both in the x and y directions into cells of size Δx and Δy respectively. Similarly, the time variable is also discretized into Δt units. As a matter of notation we utilize i,j and n as indexing variables for x,y and t. For a computational domain with left corner at the origin, we have for any field component variable, Q_x,

$$Q^n_{x;i,j} = Q_x(i\Delta x, j\Delta y, n\Delta t).$$

For computational domains not placed at the origin, similar notation is obtained by applying the appropriate shift. We now choose the location of the field components spatially according to Yee's Algorithm [19]. This yields field components which are staggered spatially as shown in Fig. 2.1.

Additionally, these field components are staggered in time. That is $\mathbf{E}$ and $\mathbf{D}$ are computed at time index $n + \frac{1}{2}$ while $\mathbf{B}$ and $\mathbf{H}$ are computed at time index n. This staggered lattice yields two significant advantages. First, for each of the curl equations the derivatives are approximated at the same point in space and time. Additionally,

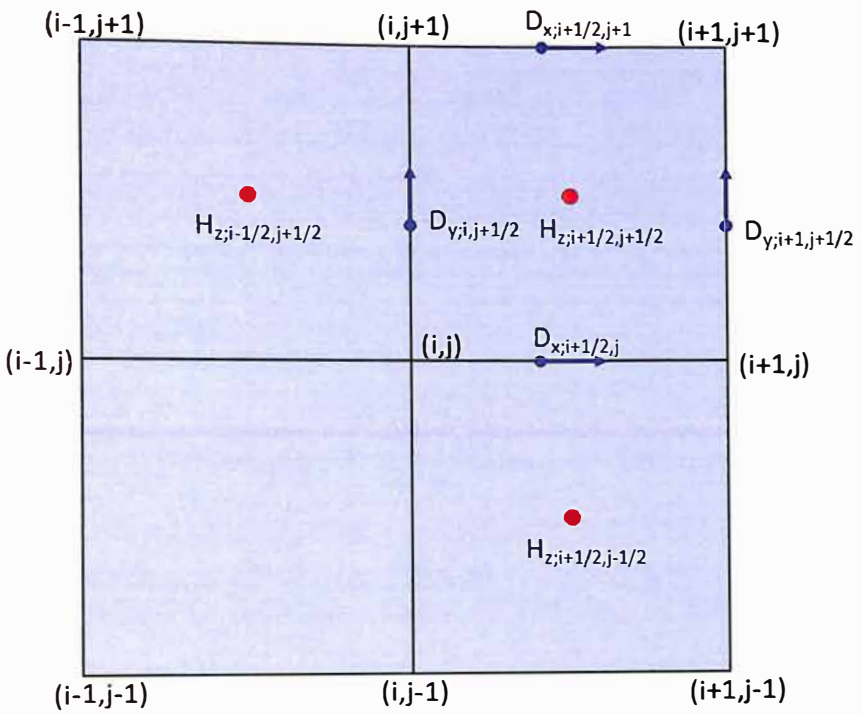

Figure 2.1: Cell location at index (i,j)

the use of such a grid is divergence free, meaning the scheme automatically satisfies Gauss' Laws of Electric (for charge free media where $\rho = 0$) and Magnetic Fields. Using central difference approximations based on this staggered grid we have

$$\frac{D^{n+\frac{1}{2}}_{x;i+\frac{1}{2},j} - D^{n-\frac{1}{2}}_{x;i+\frac{1}{2},j}}{\Delta t} = \frac{H^{n}_{z;i+\frac{1}{2},j+\frac{1}{2}} - H^{n}_{z;i+\frac{1}{2},j-\frac{1}{2}}}{\Delta y}, \tag{2.15}$$

$$\frac{D^{n+\frac{1}{2}}_{y;i,j+\frac{1}{2}} - D^{n-\frac{1}{2}}_{y;i,j+\frac{1}{2}}}{\Delta t} = \frac{H^{n}_{z;i+\frac{1}{2},j+\frac{1}{2}} - H^{n}_{z;i-\frac{1}{2},j+\frac{1}{2}}}{\Delta x} \tag{2.16}$$

and

$$\frac{B^{n+1}_{z;i+\frac{1}{2},j+\frac{1}{2}} - B^{n}_{z;i+\frac{1}{2},j+\frac{1}{2}}}{\Delta t} = \frac{E^{n+\frac{1}{2}}_{x;i+\frac{1}{2},j+1} - E^{n+\frac{1}{2}}_{x;i+\frac{1}{2},j}}{\Delta y} - \frac{E^{n+\frac{1}{2}}_{y;i+1,j+\frac{1}{2}} - E^{n+\frac{1}{2}}_{y;i,j+\frac{1}{2}}}{\Delta x}. \tag{2.17}$$

Rearranging equations (2.15), (2.16) and (2.17) yields the update equations for the flux density fields $\mathbf{D}$ and $\mathbf{B}$

$$D^{n+\frac{1}{2}}_{x;i+\frac{1}{2},j} = D^{n-\frac{1}{2}}_{x;i+\frac{1}{2},j} + \frac{\Delta t}{\Delta y}\left[H^{n}_{z;i+\frac{1}{2},j+\frac{1}{2}} - H^{n}_{z;i+\frac{1}{2},j-\frac{1}{2}}\right], \tag{2.18}$$

$$D^{n+\frac{1}{2}}_{y;i,j+\frac{1}{2}} = D^{n-\frac{1}{2}}_{y;i,j+\frac{1}{2}} + \frac{\Delta t}{\Delta x}\left[H^{n}_{z;i+\frac{1}{2},j+\frac{1}{2}} - H^{n}_{z;i-\frac{1}{2},j+\frac{1}{2}}\right] \tag{2.19}$$

and

$$\begin{aligned} B^{n+1}_{z;i+\frac{1}{2},j+\frac{1}{2}} = B^{n}_{z;i+\frac{1}{2},j+\frac{1}{2}} &+ \frac{\Delta t}{\Delta y}\left[E^{n+\frac{1}{2}}_{x;i+\frac{1}{2},j+1} - E^{n+\frac{1}{2}}_{x;i+\frac{1}{2},j}\right] \\ &- \frac{\Delta t}{\Delta x}\left[E^{n+\frac{1}{2}}_{y;i+1,j+\frac{1}{2}} - E^{n+\frac{1}{2}}_{y;i,j+\frac{1}{2}}\right]. \end{aligned} \tag{2.20}$$

If we consider an isotropic medium and apply the inverse constitutive relations (ie: $\mathbf{E} = \alpha\mathbf{D}$ and $\mathbf{H} = \gamma\mathbf{B}$)

$$E^{n+\frac{1}{2}}_{x;i+\frac{1}{2},j} = \alpha^{n+\frac{1}{2}}_{x;i+\frac{1}{2},j} D^{n+\frac{1}{2}}_{x;i+\frac{1}{2},j}, \tag{2.21}$$

$$E_{y;i,j+\frac{1}{2}} = \alpha^{n+\frac{1}{2}}_{y;i,j+\frac{1}{2}} D^{n+\frac{1}{2}}_{y;i,j+\frac{1}{2}}, \tag{2.22}$$

$$H^{n+1}_{z;i+\frac{1}{2},j+\frac{1}{2}} = \gamma^{n+1}_{z;i+\frac{1}{2},j+\frac{1}{2}} B^{n+1}_{z;i+\frac{1}{2},j+\frac{1}{2}}. \tag{2.23}$$

These update equations form the foundation of the FDTD method. The overall algorithm is as follows

Algorithm 1 2D FDTD Algorithm for Isotropic materials

```
Initialize D,E,B and H fields
for each time step do
    for each spatial step in the x direction do
        for each spatial step in the y direction do
            Update D fields using equations (2.18) and (2.19)
            Update E fields using equations (2.21) and (2.22)
        end for
    end for
    Increment time step by 1/2
    for each spatial step in the x direction do
        for each spatial step in the y direction do
            Update B field using equation (2.20)
            Update H field using equation (2.23)
        end for
    end for
end for
```

We note that while the algorithm is presented using "for loops", the spatial loops are both parallaelizable and vectorizable.

2.2.2 FDTD for Anistropic media

While the FDTD algorithm was originally designed for the numerical simulation of electromagnetic waves in isotropic medium, the FDTD algorithm has since been extended to stably simulate anisotropic media [16, 17].

If we consider the relevant constitutive relations for 2-D anisotropic in component form, we have

$$E_x = \xi_{xx} D_x + \xi_{xy} D_y, \tag{2.24}$$

$$E_y = \xi_{yy} D_y + \xi_{xy} D_x \tag{2.25}$$

and

$$H_z = \gamma B_z. \tag{2.26}$$

Creating update equations from these we obtain

$$E^{n+\frac{1}{2}}_{x;i+\frac{1}{2};j} = \xi^{n+\frac{1}{2}}_{xx;i+\frac{1}{2},j} D^{n+\frac{1}{2}}_{x;i+\frac{1}{2},j} + \xi^{n+\frac{1}{2}}_{xy;i+\frac{1}{2},j} D^{n+\frac{1}{2}}_{y;i+\frac{1}{2},j}, \tag{2.27}$$

$$E^{n+\frac{1}{2}}_{y;i;j+\frac{1}{2}} = \xi^{n+\frac{1}{2}}_{xx;i,j+\frac{1}{2}} D^{n+\frac{1}{2}}_{x;i,j+\frac{1}{2}} + \xi^{n+\frac{1}{2}}_{xy;i,j+\frac{1}{2}} D^{n+\frac{1}{2}}_{y;i,j+\frac{1}{2}}. \tag{2.28}$$

However, since the x and y components of the field are not collocated on the Yee grid, they must be approximated. The method presented in [16] utilizes a symmetric average scheme which results in stable simulation of anisotropic materials. This scheme is depicted in Fig. 2.2.

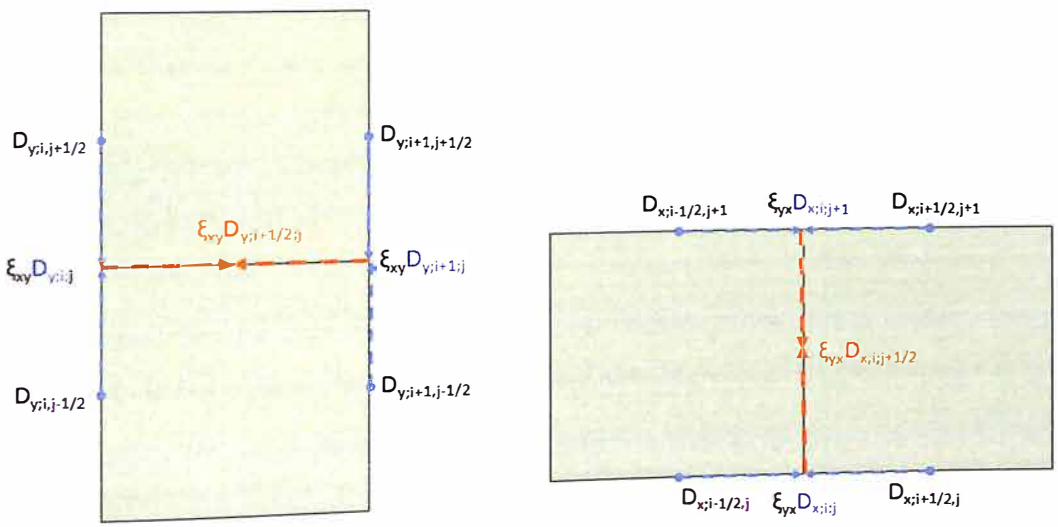

Figure 2.2: Stable averaging scheme for anisotropic media

First, the known D values from two adjacent cells are averaged towards corners of the cell intersection as shown in blue. Next ξD is computed at these points and averaged to arrive at the desired grid location. This method provides some insight into the extendability of the Yee algorithm as well as provides a starting point for extensions to 2-D anisotropic magneto-electric materials as will be discussed as a possible future work in Chapter 5.

Chapter 3

TRANSFORMATION OPTICS AND MAGNETO-ELECTRIC MEDIA

With recent research in the area of meta-materials, man-made materials constructed from sub-wavelength building blocks, new and exciting ways to alter electromagnetic waves have been uncovered. Transformation Optics is a technique for designing complicated optical devices that can make use of the versatility of meta-materials [15]. Using this technique, cylindrical spatial cloaks [9], optical waveguides [18] and space-time cloaks [8] have been designed.

The design paradigm behind Transformation Optics is as follows. First, the behavior of an electromagnetic device is considered. This behavior is viewed as a transformation of free-space with regard to how it alters electromagnetic field lines or wave trajectories. This transformation is determined mathematically usually through geometric means and then applied to Maxwell's equations. From this application and the form invariance of Maxwell's equations, the material parameters necessary to construct a device with the behavior modeled by the transformation are revealed. We briefly review the theory behind Transformation optics.

3.1 Transformations of Maxwell's Equations

We start by considering the effect of applying a transformation to Maxwell's Equations. For convenience we write Maxwell's equations in the covariant form. To facilitate this we define the space-time derivative operator

$$\hat{\nabla} = (\frac{\partial}{\partial t}, \frac{\partial}{\partial x}, \frac{\partial}{\partial y}, \frac{\partial}{\partial z}) \tag{3.1}$$

as well as the following Maxwell bi-vectors or electromagnetic tensors

$$\hat{M} = \begin{pmatrix} 0 & D_x & D_y & D_z \\ -D_x & 0 & H_z & -H_y \\ -D_y & -H_z & 0 & H_x \\ -D_z & H_y & -H_x & 0 \end{pmatrix} \tag{3.2}$$

and

$$\hat{N} = \begin{pmatrix} 0 & B_x & B_y & B_z \\ -B_x & 0 & -E_z & E_y \\ -B_y & E_z & 0 & -E_x \\ -B_z & -E_y & E_x & 0 \end{pmatrix}. \tag{3.3}$$

Using these matrices and the space-time derivative operator we can express Maxwell's equation in the covariant form. Utilizing $\hat{\nabla}$ and $\hat{M}$ yields the covariant formulation of Gauss's Law of Electric fields and Ampere-Maxwell's Law,

$$\hat{\nabla}\hat{M} = 0, \tag{3.4}$$

while using $\hat{\nabla}$ and N yields the formulation for Gauss's Law of Magnetic fields and Faraday's Law,

$$\hat{\nabla}\hat{N} = 0. \tag{3.5}$$

The fundamental idea of Transformation optics is grounded in the fact that these equations are invariant under transformations. That is when a transformation $T : (t, x, y, z) \rightarrow (\tau, \xi, \eta, \zeta)$ given by

$$\tau = \tau(t, x, y, z), \tag{3.6}$$

$$\xi = \xi(t, x, y, z), \tag{3.7}$$

$$\eta = \eta(t, x, y, z), \tag{3.8}$$

$$\zeta = \zeta(t, x, y, z) \tag{3.9}$$

with Jacobian $\hat{\Lambda}$,

$$\hat{\Lambda} = \begin{pmatrix} t_\tau & t_\xi & t_\eta & t_\zeta \\ x_\tau & x_\xi & x_\eta & x_\zeta \\ y_\tau & y_\xi & y_\eta & y_\zeta \\ z_\tau & z_\xi & z_\eta & z_\zeta \end{pmatrix} \tag{3.10}$$

is applied to Maxwell's Equations, the resulting system has the same form. Hence in the new coordinate system, Maxwell's equation is given by

$$\hat{\nabla}' \hat{M}' = 0, \tag{3.11}$$

$$\hat{\nabla}' \hat{N}' = 0 \tag{3.12}$$

where

$$\hat{\nabla}' = (\frac{\partial}{\partial \tau}, \frac{\partial}{\partial \xi}, \frac{\partial}{\partial \eta}, \frac{\partial}{\partial \zeta}), \tag{3.13}$$

$$\hat{M}' = \begin{pmatrix} 0 & D_\xi & D_\eta & D_\zeta \\ -D_\xi & 0 & H_\zeta & -H_\eta \\ -D_\eta & -H_\zeta & 0 & H_\xi \\ -D_\zeta & H_\eta & -H_\xi & 0 \end{pmatrix} \tag{3.14}$$

and

$$\hat{N}' = \begin{pmatrix} 0 & B_\xi & B_\eta & B_\zeta \\ -B_\xi & 0 & -E_\zeta & E_\eta \\ -B_\eta & E_\zeta & 0 & -E_\xi \\ -B_\zeta & -E_\eta & E_\xi & 0 \end{pmatrix}, \tag{3.15}$$

with the relationship between the coordinate systems being given by

$$\hat{M}' = |\hat{\Lambda}|\hat{\Lambda^{-1}}\hat{M}\hat{\Lambda}^{-T}, \tag{3.16}$$

$$\hat{N}' = |\hat{\Lambda}|\hat{\Lambda^{-1}}\hat{M}\hat{\Lambda}^{-T}. \tag{3.17}$$

3.1.1 Transformed material parameters for spatial transformations

If we consider a purely spatial transformation with Jacobian

$$\hat{\Lambda} = \begin{pmatrix} 1 & 0 \\ 0 & \Lambda \end{pmatrix} \tag{3.18}$$

then from [15], then a relationship between the material parameters and field quantities in both coordinate systems can be established by

$$\epsilon' = |\Lambda|\Lambda^{-1}\epsilon\Lambda^{-T}, \tag{3.19}$$

$$\mu' = |\Lambda|\Lambda^{-1}\mu\Lambda^{-T}, \tag{3.20}$$

$$\begin{pmatrix} E_\xi \\ E_\eta \\ E_\zeta \end{pmatrix} = \Lambda^T \begin{pmatrix} E_x \\ E_y \\ E_z \end{pmatrix} \tag{3.21}$$

and

$$\begin{pmatrix} H_\xi \\ H_\eta \\ H_\zeta \end{pmatrix} = \Lambda^T \begin{pmatrix} H_x \\ H_y \\ H_z \end{pmatrix}. \tag{3.22}$$

Equations (3.19) and (3.20) form the basis of Transformation Optics. When a electromagnetic device's behavior is viewed as a transformation, these equations allow us to determine the exact material parameters needed to replicate that behavior.

3.1.2 Material parameters for a 1D space-time transformation (1+1D)

If we consider the 1-D case, further work, [8], shows that for a 1+1D transformation $(t, x, y, z) \rightarrow (\tau, \xi, \eta, \zeta)$

$$\tau = \tau(t, x), \tag{3.23}$$

$$\xi = \xi(t, x), \tag{3.24}$$

$$\eta = y, \tag{3.25}$$

$$\zeta = z \tag{3.26}$$

with Jacobian

$$\begin{pmatrix} \Lambda & 0 \\ 0 & I_{2\times 2} \end{pmatrix} \tag{3.27}$$

the medium corresponding to the transformation is magneto-electric. The fundamental relationship between the transformation and material parameters is given by the matrix equations

$$\begin{pmatrix} E_\eta & E_\zeta \\ H_\zeta & -H_\eta \end{pmatrix} = \begin{pmatrix} \frac{1}{a_{12}} & -\frac{a_{11}}{a_{12}} \\ -\frac{a_{11}}{a_{12}} & \frac{a_{12}a_{21}-a_{11}a_{22}}{a_{12}} \end{pmatrix} \begin{pmatrix} D_\eta & D_\zeta \\ H_\zeta & -H_\eta \end{pmatrix} \tag{3.28}$$

where a_{ij} are the coefficients of matrix A which is determined by the Jacobian, Λ, of the transformation T. In particular, we have

$$A = \Lambda^{-1} \begin{pmatrix} 0 & \epsilon \\ 1/\mu & 0 \end{pmatrix} \Lambda. \tag{3.29}$$

This particular medium is of interest as it directly applies to the space-time cloak. Unfortunately, implementing this medium using FDTD is not straightforward.

3.2 The conventional FDTD method for time dependent magneto-electric medium

Consider the following 1+1 D Maxwell's equations for TE_z mode

$$\frac{\partial D_z}{\partial t} = \frac{\partial H_y}{\partial x}, \tag{3.30}$$

$$\frac{\partial B_y}{\partial t} = \frac{\partial E_z}{\partial x}, \tag{3.31}$$

where the constitutive equations are given by

$$E_z = \alpha D_z + \beta B_y, \tag{3.32}$$

$$H_y = \beta D_z + \gamma B_y, \tag{3.33}$$

where α, β, and γ are space and time dependent.

We note that the primary issue with simulating magneto-electric media arises from the more complicated constitutive relations given in equations (3.32) and (3.33). Using the conventional FDTD method, the discretized Maxwell's equations (the D first scheme) are

$$D_i^{n+\frac{1}{2}} = D_i^{n-\frac{1}{2}} + \frac{\Delta t}{\Delta x}\left(H_{i+\frac{1}{2}}^n - H_{i-\frac{1}{2}}^n\right), \tag{3.34}$$

$$B_{i+\frac{1}{2}}^{n+1} = B_{i+\frac{1}{2}}^n + \frac{\Delta t}{\Delta x}\left(E_{i+1}^{n+\frac{1}{2}} - E_i^{n+\frac{1}{2}}\right), \tag{3.35}$$

and the constitutive relations (assuming that the coupled constitutive relations respond locally in space and time) become

$$E_i^{n+\frac{1}{2}} = \alpha_i^{n+\frac{1}{2}} D_i^{n+\frac{1}{2}} + \beta_i^{n+\frac{1}{2}} B_i^{n+\frac{1}{2}}, \tag{3.36}$$

$$H_{i+\frac{1}{2}}^{n+1} = \beta_{i+\frac{1}{2}}^{n+1} D_{i+\frac{1}{2}}^{n+1} + \gamma_{i+\frac{1}{2}}^{n+1} B_{i+\frac{1}{2}}^{n+1}. \tag{3.37}$$

Parameters α, β, and γ are computed analytically from equation (3.28) and are thus available at any point (t, x) in the computational domain. However, the quantities $B_i^{n+\frac{1}{2}}$ in equation (3.36) and $D_{i+\frac{1}{2}}^{n+1}$ in equation (3.37) are not computed in the discretized Maxwell's equations, equation (3.34) and (3.35).

As a result, the conventional Yee approach cannot be directly used in the simulation of magneto-electric media. One method for resolving these issues is to use time extrapolation and space interpolation. To compute $B_i^{n+\frac{1}{2}}$ in equation (3.36), we have with time extrapolation

$$B_i^{n+\frac{1}{2}} \approx \frac{3B_i^n - B_i^{n-1}}{2}. \tag{3.38}$$

Applying spatial interpolation yields

$$B_i^{n+\frac{1}{2}} \approx \frac{\frac{3}{2}(B_{i+\frac{1}{2}}^n + B_{i-\frac{1}{2}}^n) - \frac{1}{2}(B_{i+\frac{1}{2}}^{n-1} + B_{i-\frac{1}{2}}^{n-1})}{2} \tag{3.39}$$

$$\approx \frac{3B_{i+\frac{1}{2}}^n + 3B_{i-\frac{1}{2}}^n - B_{i+\frac{1}{2}}^{n-1} - B_{i-\frac{1}{2}}^{n-1}}{4}, \tag{3.40}$$

which is valid after the first timestep. For the initial timestep, we use B_i^n as an approximation for $B_i^{n+\frac{1}{2}}$. Similarly, we compute $D_{i+\frac{i}{2}}^{n+1}$ in equation (3.37) as follows

$$D_{i+\frac{1}{2}}^{n+1} \approx \frac{3D_{i+1}^{n+\frac{1}{2}} + 3D_i^{n+\frac{1}{2}} - D_{i+1}^{n-\frac{1}{2}} - D_i^{n-\frac{1}{2}}}{4}. \tag{3.41}$$

Numerical simulation of the space-time cloak shows that the conventional FDTD method presented in this section is unstable. This is primarily due to the use of time extrapolation. To avoid such extrapolation, we propose an overlapping Yee algorithm for time dependent magneto-electric media as described in the next section.

3.3 The overlapping Yee Algorithm for time dependent magneto-electric media

Rather than a single D first scheme or B first scheme, we use a combination of both. While computationally more expensive, this produces D and B values at every half time step and spatial step within our computational domain. As a result, we are able to perform the required magneto-electric Maxwell constitutive relation updates without extrapolation.

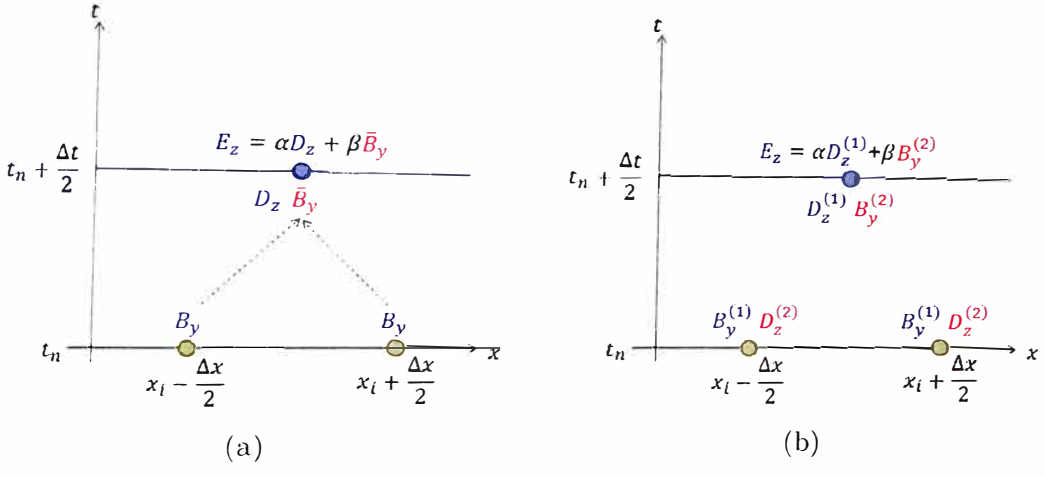

Figure 3.1: Computation of E_z using (a) the time extrapolation under a conventional FDTD method and (b) the overlapping Yee algorithm without extrapolation.

Figure 3.1 illustrates the fundamental differences between utilizing a conventional FDTD approach and the overlapping grid approach. Figure 3.1(a) depicts that, due to the coupled constitutive relations, at any given step, E_z has a dependence on the quantity $\overline{B_y}$. The dotted arrows leading to this value indicate that $\overline{B_y}$ must be extrapolated in time and interpolated in space from values known on the conventional FDTD grid.

On the other hand, Fig. 3.1(b) illustrates that by utilizing a dual overlapping grid approach, the dependence on time extrapolation and spatial interpolation can be eliminated. A new superscript notation is used to indicate the usage of two overlapping grids and to specify which grid each value of B_y and E_z comes from. All values needed to compute E_z at a particular instance in time exists on one of the two grids.

In presenting an algorithm for the adjusted scheme we utilize the convention that n represents the time coordinate of the grid point and i represents the spatial coordinate. Indices of $n \pm \frac{1}{2}$ and $i \pm \frac{1}{2}$ are use to represent locations that are a half time step or spatial step from the gridpoint. With this established, we present an algorithm for an overlapping Yee FDTD method.

The algorithm in 1D case can be summarized by the following steps:

1. *Update* $D_i^{n+\frac{1}{2}}$ *on the first Yee grid and* $B_i^{n+\frac{1}{2}}$ *on the second Yee grid:*

$$D_i^{n+\frac{1}{2}} = D_i^{n-\frac{1}{2}} + \frac{\Delta t}{\Delta x}\left[H_{i+\frac{1}{2}}^n - H_{i-\frac{1}{2}}^n\right],$$

$$B_i^{n+\frac{1}{2}} = B_i^{n-\frac{1}{2}} + \frac{\Delta t}{\Delta x}\left[E_{i+\frac{1}{2}}^n - E_{i-\frac{1}{2}}^n\right].$$

2. *Update* $E_i^{n+\frac{1}{2}}$ *and* $H_i^{n+\frac{1}{2}}$*:*

$$E_i^{n+\frac{1}{2}} = \alpha_i^{n+\frac{1}{2}} D_i^{n+\frac{1}{2}} + \beta_i^{n+\frac{1}{2}} B_i^{n+\frac{1}{2}},$$

$$H_i^{n+\frac{1}{2}} = \beta_i^{n+\frac{1}{2}} D_i^{n+\frac{1}{2}} + \gamma_i^{n+\frac{1}{2}} B_i^{n+\frac{1}{2}}.$$

3. *Update* $B_{i+\frac{1}{2}}^{n+1}$ *on the first Yee grid and* $D_{i+\frac{1}{2}}^{n+1}$ *on the second Yee grid:*

$$B_{i+\frac{1}{2}}^{n+1} = B_{i+\frac{1}{2}}^{n} + \frac{\Delta t}{\Delta x}\left[E_{i+1}^{n+\frac{1}{2}} - E_{i}^{n+\frac{1}{2}}\right],$$

$$D_{i+\frac{1}{2}}^{n+1} = D_{i+\frac{1}{2}}^{n} + \frac{\Delta t}{\Delta x}\left[H_{i+1}^{n+\frac{1}{2}} - H_{i}^{n+\frac{1}{2}}\right].$$

4. *Update* $E_{i+\frac{1}{2}}^{n+1}$ *and* $H_{i+\frac{1}{2}}^{n+1}$*:*

$$E_{i+\frac{1}{2}}^{n+1} = \alpha_{i+\frac{1}{2}}^{n+1} D_{i+\frac{1}{2}}^{n+1} + \beta_{i+\frac{1}{2}}^{n+1} B_{i+\frac{1}{2}}^{n+1},$$

$$H_{i+\frac{1}{2}}^{n+1} = \beta_{i+\frac{1}{2}}^{n+1} D_{i+\frac{1}{2}}^{n+1} + \gamma_{i+\frac{1}{2}}^{n+1} B_{i+\frac{1}{2}}^{n+1}.$$

We note that the extension to 2-D and 3-D should be feasible by utilizing a time collocated grid (where B and E are computed at the same instance in time, but not necessarily in space). Doing so eliminates time extrapolation in 2-D and 3-D but still uses interpolation in space.

Chapter 4
SIMULATION OF THE SPACETIME CLOAK

The simulation of magneto-electric media has direct applications to the spacetime cloak presented in [8]. In this chapter we create a similar diamond shaped space-time cloak using the transformation depicted in Fig. 4.1 and simulate using both the time extrapolation method and overlapping grid method.

4.1 Transformation Optics and space-time cloak

We consider a spacetime cloak design similar to the spacetime cloaks proposed in [4, 8]. Figure 4.1 shows a diamond shaped spacetime cloak in the (t, x) domain and the transformed (τ, ξ) free space. The original and the transformed regions are the same parallelograms centered at (t_0, x_0) so we have $\xi_0 = x_0$, $\tau_0 = t_0$, $\tau_p = t_p$, and $\tau_q = t_q$. In the parallelogram we apply the following coordinate transformation to create such a spacetime cloak:

$$\tau = t, \tag{4.1}$$

$$\xi = \frac{\sigma(x - x_S)}{\sigma - \delta(t - t_S)/(t_0 - t_S)} + x_S, \tag{4.2}$$

where the values of x_S and t_S depend on the region where (t, x) lies in:

$$t_S = \begin{cases} t_p, & \text{if } (t, x) \text{ lies in region I or II,} \\ t_q, & \text{if } (t, x) \text{ lies in region III or IV,} \end{cases} \tag{4.3}$$

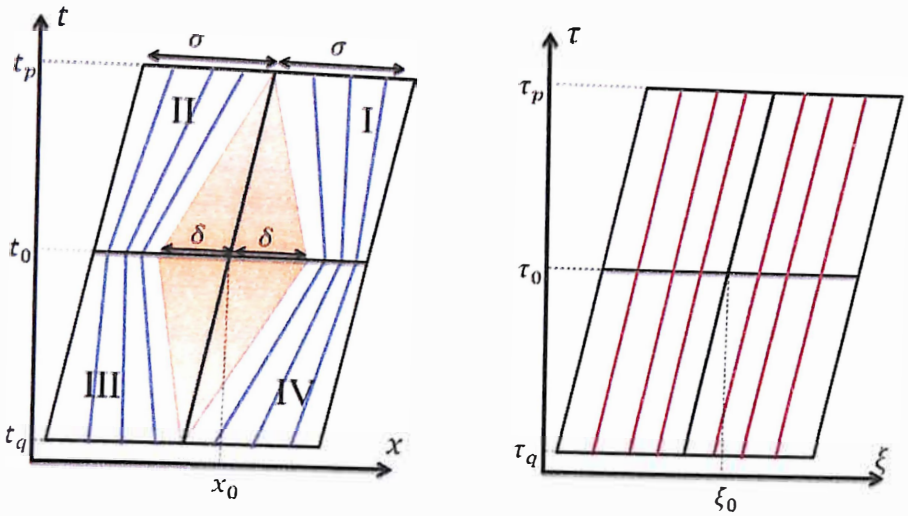

(a) (b)

Figure 4.1: (a) A spacetime cloak in the (t, x) domain. (b) Free space after the transformation to the (τ, ξ) domain.

and

$$x_S = \begin{cases} x_0 + (t - t_0)c + \sigma, & \text{if } (t, x) \text{ lies in region I or IV,} \\ x_0 + (t - t_0)c - \sigma, & \text{if } (t, x) \text{ lies in region II or III.} \end{cases} \tag{4.4}$$

4.2 Simulation of the space-time cloak

In simulating the above cloak, we utilize a 10 μm by 15 fs long computational domain with a plane wave (with $\lambda = 600\ nm$) traveling in the positive x direction. Our spacetime cloak is 1200 nm wide and lasts 6 fs. With regards to Fig. 4.1(a) we have $x_0 = 1.5\ \mu m$, $t_0 = 9\ fs$, $t_q = 6\ fs$, $t_p = 12\ fs$, $\sigma = 600\ nm$ and $\delta = 180\ nm$. The computational domain is terminated by perfectly matched layer (PML) absorbing boundary conditions [13]. Due to the fast and slow phase velocities in the spacetime cloak [8], Δt is chosen by $\Delta t \leq \Delta x / v_{max}$ where v_{max} is the largest wave speed

computed in the cloaking region. We perform the simulation 3 times with the number of spatial cells, N, equal to 1600, 2000, and 2400 and the same number of time steps.

The numerical simulation results are shown in Fig. 4.2. The figures shown are contour plots of the intensity of the electric field generated by the interaction between the incident source and the spacetime cloak. We compare the conventional FDTD method with time extrapolation and the proposed overlapping Yee FDTD method for various spatial resolutions. The result shows the bending of the electric field (and consequently the electromagnetic wave) in space and time around the cloaked event. The shown simulation results verify that an extrapolation approach is unstable (near the closing process of the cloaked event) and the proposed overlapping FDTD approach provides stable results.

We now examine the behavior of the electric field as the wave propagates through the diamond shaped space-time region under the same simulation parameters. As the wave enters the cloak it begins to split as the front portion of the wave speeds up and the back portion of the wave slows down. This effect is made possible due to the space-time dependence of the media within the cloaking region. As this separation occurs, it is mirrored in the electric field producing a gap in the electric field. The early development of this gap is shown in Fig. 4.3(a) near $x = 1000\ nm$. As the wave progresses through the media, the cloak widens in the x direction allowing for the size of this gap to increase as time progresses. The gap in the electric field, as shown in Fig. 4.3(b), is at a maximum at the center of the cloaking region. As the wave propagates past this point, the cloak begins to close (shrink in the x direction). Due to the closing of the cloak, the front of the wave begins to slow down while the back speeds up. This action allows for the wave to remerge just as it exits

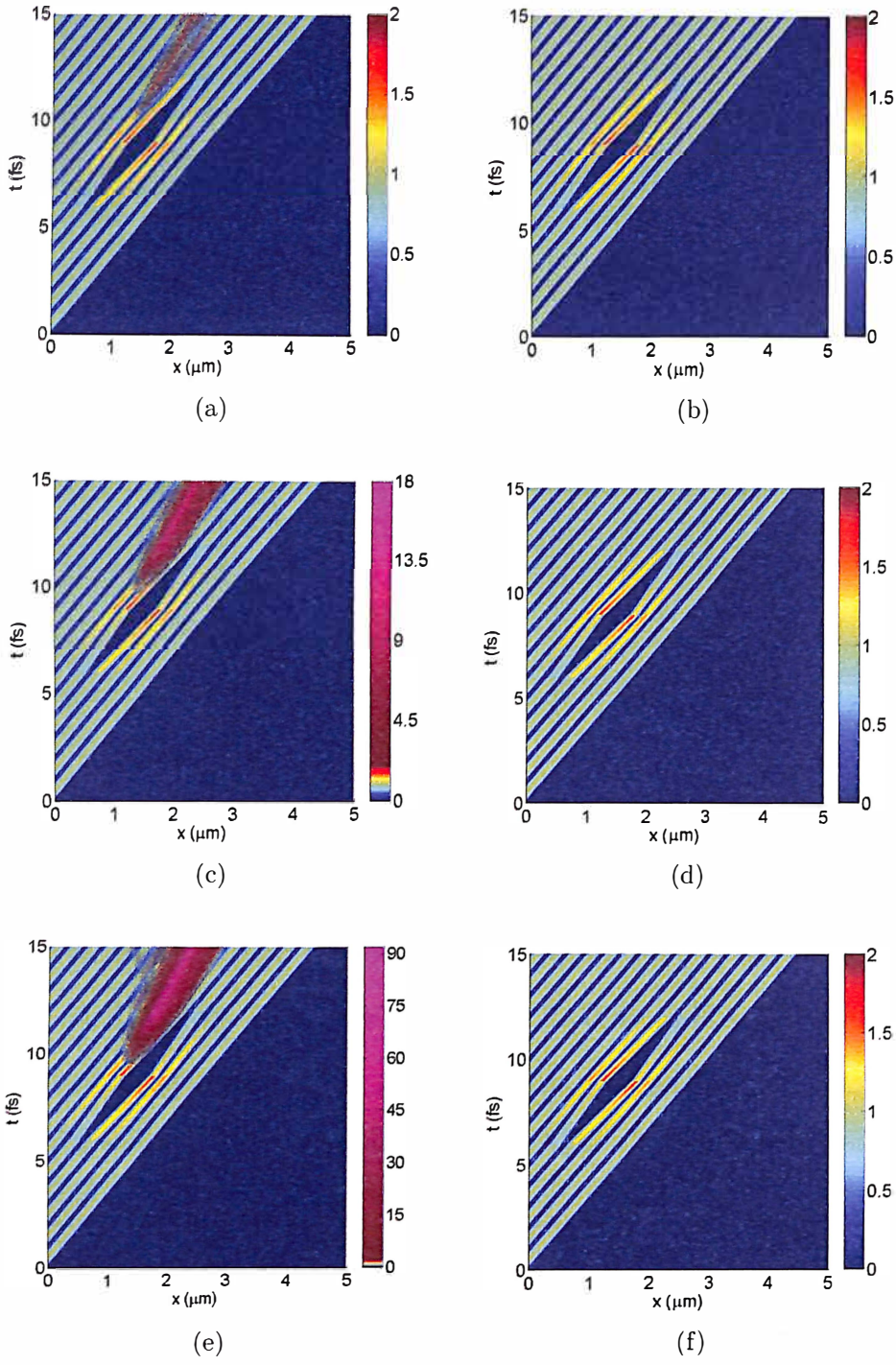

Figure 4.2: Contour plots of the electric field intensity for spacetime cloak simulations. Left column: results using a conventional time extrapolation based FDTD method with grid sizes a) $N = 1600$, (c) $N = 2000$, and (e) $N = 2400$, respectively. Right column: the corresponding results using the overlapping Yee FDTD method.

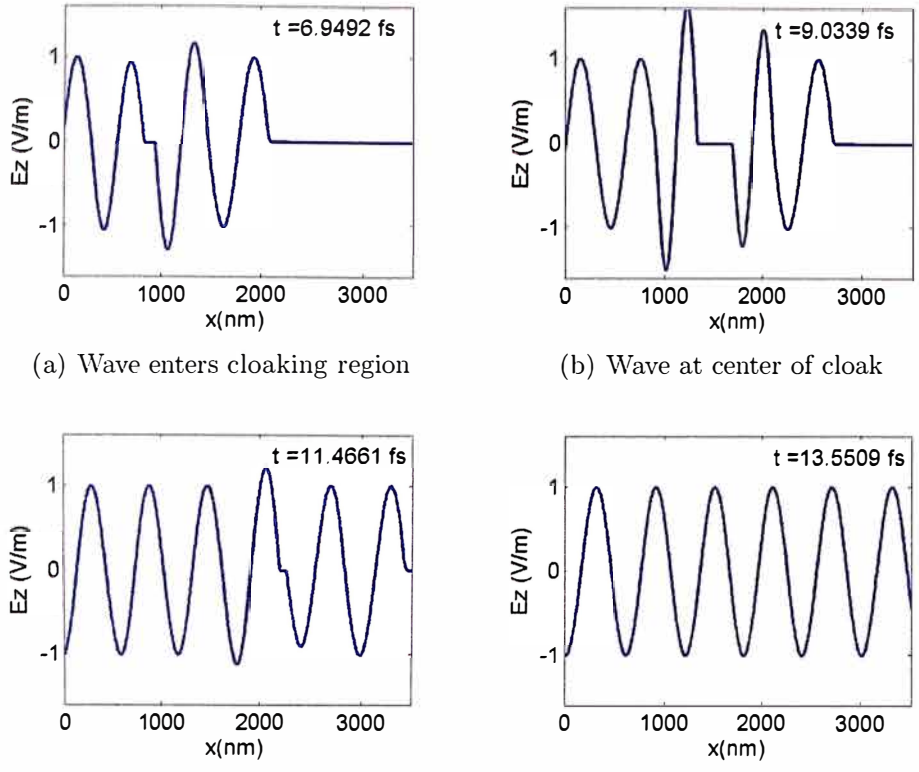

(a) Wave enters cloaking region

(b) Wave at center of cloak

(c) Wave leaving cloaking region

(d) Wave after leaving cloak

Figure 4.3: Evolution of the Electric field as the wave propagates through the space-time cloak.

the cloak. The field behavior moments before the wave exits the cloak is shown in Fig. 4.3(c). At this point a small gap near $x = 2200\ nm$ still exists. Once the wave has propagated through the cloak region, it is fully rejoined and the propagation behavior and resulting field behavior returns to that of propagation in an isotropic media, as shown in Fig. 4.3(d).

4.3 Stability Analysis

To conduct a stability analysis, we compare the distribution of eigenvalues of the conventional FDTD method to that of our overlapping grid approach with respect

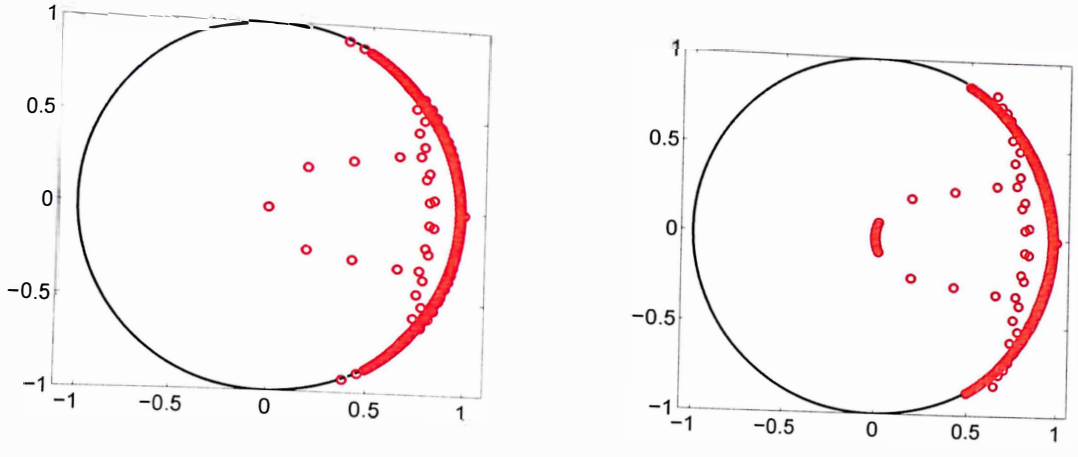

(a) (b)

Figure 4.4: Distribution of the eigenvalues in the complex plane for (a) the overlapping Yee FDTD method and (b) the conventional FDTD method.

to the unit circle. For both tests we utilize similar simulation parameters as in the previous section, but with a smaller mesh size of $N = 200$. We compute the eigenvalues of the numerical update equations at a time instant when $t \in (t_q, t_p)$ and plot them in the complex plane. The results when $t = 8.34\ fs$ are shown in Fig. 4.4.

As indicated in the Fig. 4.4(a) all the eigenvalues of the overlapping approach lie within or on the unit circle with the ones lying on unit circle being simple eigenvalues. On the other hand, Fig. 4.4(b) shows that some of eigenvalues (near the upper and lower right corners) of the conventional FDTD approach lie outside the unit circle. In particular the modulus of the largest eigenvalue is 1 for the overlapping method and 1.046 for the conventional FDTD method. This indicates that the overlapping Yee FDTD method is stable while the conventional FDTD approach (with extrapolation) would experience instability.

In summary, we have proposed a stable FDTD method for the simulation of space and time dependent magneto-electric medium based on the use of two sets of overlapping Yee grids that are offset in time by a half time step. Additionally, we have shown the direct application of this method to the simulation of the spacetime cloak. The proposed method is useful in exploration of other new physical possibilities offered by metamaterials and transformation optics. These results have been published in [2].

Chapter 5

CONCLUSION AND FUTURE WORK

5.1 Conclusion

In this work, we presented an overview of Electromagnetics, FDTD and transformation optics. New work was done in area of magnetoelectric materials. In particular, we presented a stable FDTD based algorithm for the simulation of these 1-D Magneto-electric materials. As a numerical example, the 1-D space-time cloak was derived using Transformation Optics and simulated using the proposed FDTD algorithm.

5.2 Future Work

In the future we consider possible extensions to this algorithm. The most immediate is the extension to 2-D + 1. In this case we introduce the possibility of the material not only being magnetoelectric, but also anisotropic. This is a medium that has constitutive relations given by

$$D = \begin{pmatrix} \epsilon_{xx} & \epsilon_{xy} \\ \epsilon_{yx} & \epsilon_{yy} \end{pmatrix} E + \beta H \tag{5.1}$$

and

$$B = \mu H + \beta E. \tag{5.2}$$

As described in Chapter 2 and Chapter 3, the anisotropic and magnetoelectric properties of this material introduces the issue of requiring field values not included on the FDTD grid. One approach we wish to try is by combining the overlapping grid method with the method for anistropic materials proposed in [16].

REFERENCE LIST

[1] A. Akyurtlu and D. Werner. BI-FDTD: A novel finite-difference time-domain formulation for modeling wave propagation in bi-isotropic media. *IEEE Transactions on Antennas and Propagation*, 52(2):416–425, 2004.

[2] J. Cornelius, J. Liu, and M. Brio. Finite-difference time-domain simulation of spacetime cloak. *Opt. Express*, 22:12087–12095, May 2014.

[3] A. Gaeta, M. Fridman, A. Farsi, and Y. Okawachi. Demonstration of temporal cloaking. *Nature*, 481:62–65, 2012.

[4] P. Kinsler and M. McCall. Cloaks, editors, and bubbles: applications of spacetime transformation theory. *Ann. Phys.*, 526:51–62, 2014.

[5] U. Leonhardt. Optical conformal mapping. *Science*, 312:1777–1779, 2006.

[6] D. Lide, editor. *CRC Handbook of Chemistry and Physics.* CRC Press, 77th edition, 1999.

[7] J. Liu, M. Brio, Y. Zeng, A. Zakharian, W. Hoyer, S. W. Koch, and J. V. Moloney. Generalization of the FDTD algorithm for simulations of hydrodynamic nonlinear Drude model. *Journal of Computational Physics*, 229(17):5921–5932, 2010.

[8] M. McCall, A. Favaro, P. Kinsler, and Allan Boardman. A spacetime cloak, or a history editor. *J. Opt.*, 13:024003, 2011.

[9] J. B. Pendry, D. Schurig, and D. R. Smith. Controlling electromagnetic fields. *Science*, 312:1780–1782, 2006.

[10] A. Semichaevsky, A. Akyurtlu, D. Kern, D. Werner, and M. Bray. Novel BI-FDTD approach for the analysis of chiral cylinders and spheres. *IEEE Transactions on Antennas and Propagation*, 54(3):925–932, 2006.

[11] D. Shurig, J. Mock, B. Justice, S. Cummer, J. B. Pendry, and D. R. Smith. Metamaterial electromagnetic cloak at microwave frequencies. *Science*, 314:977–979, 2006.

[12] A. Taflove and M. E. Brodwin. Numerical solution of steady-state electromagnetic scattering problems using the time-dependent maxwell's equations. *IEEE Trans. Microwave Theory Tech.*, 23:623–630, Aug 1975.

[13] A. Taflove and S. Hagness. *Computational Electrodynamics: the Finite-Difference Time-Domain Method.* Artech House, 2005.

[14] F. Teixeira. Time-domain finite-difference and finite-element methods for Maxwell equations in complex media. *IEEE Transactions on Antennas and Propagation*, 56:2150–2166, 2008.

[15] D. Werner and D. Kwon. *Transformation Electromagnetics and Metamaterials.* Springer, 2014.

[16] G. Werner and J. Cary. A stable fdtd algorithm for non-diagonal, anisotropic dielectrics. *Journal of Computational Physics*, 226:1085–1111, 2007.

[17] G. Werner, J. Cary, and C. Bauer. A more accurate, stable, fdtd algorithm for electromagnetics in anisotropic dielectrics. *Journal of Computational Physics*, 255:436–455, 2013.

[18] H. Xu, H. Sun, and B. Zhang. Waveguide design and application with transformation optics. *Science China; Information Sciences*, 56, 2013.

[19] K. S. Yee. Numerical solution of initial boundary value problems involving maxwell's equations in isotropic media. *IEEE Transactions on Antennas and Propagation*, 14:302–307, 1966.

CURRICULUM VITAE

Jason Cornelius
jmcornelius10@students.desu.edu
(302)-747-6757

Department of Mathematics
Delaware State University
1200 N. Dupont Hwy.
Dover, DE 19904

Research Interests

Computational Electrodynamics, Radar Modeling, Finite-Difference Time-Domain methods, Transformation Optics.

Education

2013-2015 M.S. Degree, *Applied Mathematics*
Delaware State University
Degree Expected: August 2015.
Advisor: Dr. Jinjie Liu.

2010-2013 B.S. Degree, *Mathematics*
Delaware State University
Degree Recieved: May 2013

Publications

September 2014 *Modeling the Radar Signature of Thin Metallic Objects with the AFDTD Software*
Jason Cornelius, Traian Dogaru.
Army Research Lab,
Sensors and Electron Devices Directorate
Adelphi, MD.

Spring 2014 *Finite-difference time-domain simulation of spacetime cloak*
Jason Cornelius, Jinjie Liu, Moysey Brio
Optical Express

Related Skills

Proficient in the use of C, C++, Java, Javascript, HTML. Well-versed in Computer Algebraic Systems such as Maple and MATLAB.